Optimization of Radial Active Magnetic Bearings Using the Finite Element Technique and the Differential Evolution Algorithm

Gorazd Štumberger, Drago Dolinar, Uwe Pahner and Kay Hameyer

Abstract— **An optimization of radial active magnetic bearings is presented in the paper. The radial bearing is numerically optimized, using Differential Evolution – a stochastic direct search algorithm. The nonlinear solution of the magnetic vector potential is determined, using the 2D finite element method. The force is calculated by Maxwell's stress tensor method. The parameters of the optimized and non optimized bearing are compared. The force, the current gain, and the position stiffness are given as functions of the control current and rotor displacement.**

Keywords— **Magnetic levitation, Numerical analysis, Optimization methods, Parameter estimation.**

I. Introduction

ACTIVELY controlled magnetic bearing system is an indispensable element when we have to satisfy the machine–tool industry's demand for high-speed, high-precision machining. A typical system of Active Magnetic Bearings (AMBs) [1] consists of controlled electromagnets, used to control five degrees of freedom (DOFs), and a driving motor that controls the sixth DOF. Two pairs of radial bearings that control four DOFs are placed at each rotor end. The fifth DOF is controlled by a pair of axial bearings.

Two electromagnets on the opposite sides of the ferromagnetic rotor pull the rotor in opposite directions. The total force acting on the rotor is equal to the vector sum of forces of all electromagnets. Such system of electromagnets and ferromagnetic rotor is open loop unstable. It is stabilized by corresponding current and position control assuring the contact–less suspension of the rotor.

The total force of two electromagnets is nonlinear function of the current, the rotor position and magnetization of the iron. The nonlinear current–force dependence is efficiently linearized by bias and control current, while the position–force dependence and iron magnetization remain nonlinear. The control design is often based on a linearized dynamic model. However, the stability and the robustness of the controlled AMB system can be efficiently tested with the analysis of the linearized model in the entire operation range. The Finite Element Method (FEM) based calculations may be very helpful for this purpose [2], [3].

The design of AMBs is expected to satisfy the static and dynamic requirements in the best possible way. It can be found either by experience and trials or by applying numerical optimization methods. AMBs are nonlinear systems. The dependency of the objective function and its gradients from the design parameters is unknown. For the optimization of such constrained, nonlinear electro–mechanical problems, the use of stochastic search methods in combination with the FEM–based analysis is recommendable [4], [5].

In this paper the numerical optimization of radial AMBs using Differential Evolution (DE) [6] – a direct stochastic search algorithm – is presented. The aim is to achieve maximum force at a minimum mass of the entire construction. The objective function is evaluated by FEM–based 2D calculations. It includes the determination of the nonlinear solution of the magnetic vector potential and the determination of force by Maxwell's stress tensor method. The optimization has been performed in a special environment tuned for FEM–based numerical optimizations [7]. The linearized equations are applied to compare the performance of designs prior to and after the optimization.

II. Radial active magnetic bearing

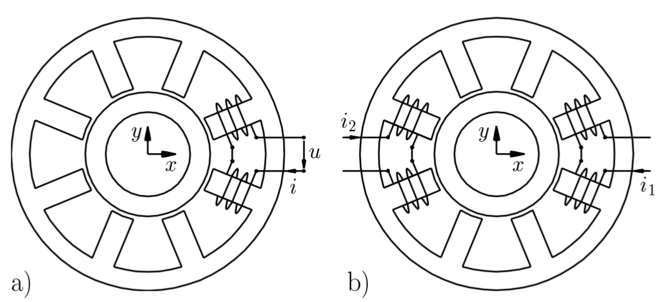

Fig. 1. An electromagnet a), a pair of electromagnets b).

The voltage balance in the coil of an electromagnet, shown in Fig. 1.a), is described by (1):

$$u = Ri + L\frac{di}{dt} + k_u\frac{dx}{dt} \qquad (1)$$

where u is the voltage, i the current, R the Ohmic resistance, L the inductance, k_u the coefficient of induced volt-

Manuscript received October 25, 1999.

The authors are grateful to the Belgian Federal office for scientific, technical and cultural affairs for promoting the W&T cooperation with Central- and Eastern Europe by giving the DWTC grant to D. Dolinar. Our thanks are due to the Slovene Ministry of Science and Technology for the financial support.

Gorazd Štumberger, E-mail: gorazd.stumberger@uni-mb.si and Drago Dolinar, E-mail: dolinar@uni-mb.si, are with the Faculty of Electrical Engineering and Computer Science, Smetanova 17, 2000 Maribor, Slovenia.

Uwe Pahner, E-mail: uwe.pahner@east.kuleuven.ac.be and Kay Hameyer, E-mail: kay.hameyer@east.kuleuven.ac.be, are with the Katholieke Universiteit Leuven, Dept. E.E.(ESAT), Div. ELEN, Kardinaal Mercierlaan 94, B-3001 Leuven, Belgium.

age, and $\frac{dx}{dt}$ the derivative of the rotor displacement in the axis x. The current through the coil of the electromagnet generates the attractive force. It attracts the ferromagnetic rotor to the core of the electromagnet. In general, pairs of electromagnets are used in magnetic bearings as presented in Fig. 1.b). The force of a pair of electromagnets in the same magnetic bearing axis depends on the flux densities in the air gaps of both electromagnets (2):

$$F = k\frac{B_1^2}{\mu_0}A - k\frac{B_2^2}{\mu_0}A \quad (2)$$

where k is the geometric factor (for an eight–pole bearing $k = \cos(\pi/8)$), B_1 and B_2 are the flux densities in the air gap of the first and second electromagnet on the same bearing axis, μ_0 is the permeability of vacuum, and A is the area of one pole. The flux densities B_1 and B_2 are caused by the currents i_1 and i_2. If the nonlinearity of iron is neglected (2) can be transformed to (3):

$$F = \frac{k\mu_0(Ni_1)^2}{4(\delta - x)^2}A - \frac{k\mu_0(Ni_2)^2}{4(\delta + x)^2}A \quad (3)$$

where Ni_1 and Ni_2 are the magnetomotive forces of electromagnets on the same bearing axis that generate the attraction forces acting on the rotor in opposite directions, and δ is the air gap. Let us introduce the bias current i_b and the control current i_p. The same bias current i_b is supplied into the coils of both electromagnets. Force control is done by adding a control current i_p into the coil of one electromagnet and subtracting it in the coil of other one (4):

$$i_1 = i_b + i_p \qquad \text{and} \qquad i_2 = i_b - i_p \quad (4)$$

where $i_p \leq i_b$. The relation between the control current and the resultant force is obtained by inserting expressions (4) into (3):

$$F = \frac{k\mu_0 N^2(i_b + i_p)^2}{4(\delta - x)^2}A - \frac{k\mu_0 N^2(i_b - i_p)^2}{4(\delta + x)^2}A \quad (5)$$

Equation (6) is obtained by rearranging (5). It expresses the linear dependence between resultant force and control current i_p.

$$F = \frac{k\mu_0 AN^2 i_b}{2(\delta - x)^2}i_p \quad (6)$$

Equation (5) can be linearized about the operating point $x = x_0$, $i_p = i_{p0}$. The so obtained equation (7) is valid exclusively close about the point of linearization. The expression $F(x, i_p)$ represents the functional dependence of the force on the rotor displacement x and the control current i_p, while the expression $F(x_0, i_{p0})$ denotes the force in the operating point x_0, i_{p0}.

$$F(x, i_p) = F(x_0, i_{p0}) + k_i(i_p - i_{p0}) + k_x(x - x_0) \quad (7)$$

In the point $x = x_0$, $i_p = i_{p0}$ the current gain k_i is defined by (8), and the position stiffness k_x is given by (9):

$$k_i := \frac{\partial F(x, i_p)}{\partial i_p} \quad \text{for} \quad x = x_0; i_p = i_{po} \quad (8)$$

$$k_x := -\frac{\partial F(x, i_p)}{\partial x} \quad \text{for} \quad x = x_0; i_p = i_{po} \quad (9)$$

For $x = 0$ and $i_p = 0$ we get:

$$k_i = k\mu_0 N^2 A\frac{i_b}{\delta^2} \qquad \text{and} \qquad k_x = -k\mu_0 N^2 A\frac{i_b^2}{\delta^3}$$

The motion of the mass point with the mass m between two electromagnets located in the same axis of an AMB is described by (10).

$$F = m\frac{d^2x}{dt^2} \quad (10)$$

One axis of the radial magnetic bearing is mathematically described by the pair of voltage equations (1), by the force equation (2) and the equation of motion (10). In the vicinity of the operating point the force equation (2) can be replaced by the linearized expression (7).

Further on, the procedure for optimizing radial magnetic bearing is described. Included is the comparison of forces F, current gains k_i and the position stiffnesses k_x of the optimized and non–optimized bearing calculated for different rotor displacements $x = x_0$ and control currents $i_p = i_{p0}$.

III. Optimization

The optimization of the radial magnetic bearing, carried out in a special environment tuned for FEM–based numerical optimizations [7], is briefly described in the following six steps:

• **Step 1:** The geometry of the bearing is described parametrically and the initial parameter values are determined by a first analytical design. The bearing geometry parameters are: the stator yoke s_y, the rotor yoke r_y, the leg width l_w (all shown in Fig. 2.a)) and the bearing axial length l.

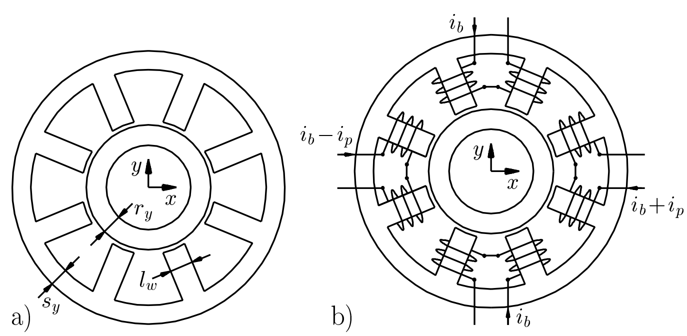

Fig. 2. The bearing geometry a), coils and currents b).

• **Step 2:** The new parameter values are determined by DE [6]. The electromagnets in the y axis are supplied by the current i_b, while the electromagnets in the x axis are supplied by the currents $i_b + i_p$ and $i_b - i_p$ at $i_p = i_b$, as shown in Fig. 2.b).

• **Step 3:** The bearing geometry, the material, the current densities and the boundary conditions are defined. The procedure continues with **Step 2** if the parameters of the bearing are outside the geometrical constraints.

• **Step 4:** First, the mesh is generated. Then the nonlinear solution of the magnetic vector potential is determined, using the conjugate gradient algorithm and

Newton-Raphson's algorithm. The 2D problem is described by (11)

$$\nabla \cdot (\nu \nabla \mathcal{A}) = -j \qquad (11)$$

where $\mathcal{A}$ is the magnetic vector potential, ν is the magnetic reluctivity, j is the applied current density, and ∇ is the Laplace operator. The whole procedure consists of the calculation of the magnetic vector potential, the analysis of errors, mesh refinement, and the repeated potential calculation.

• **Step 5:** The force is calculated by Maxwell's stress tensor method (12):

$$F = \oint_S \sigma \, dS = \oint_S \left[\frac{1}{\mu_0}(B \cdot n)B - \frac{1}{2\mu_0} B^2 n \right] dS \qquad (12)$$

where σ is the Maxwell's stress tensor, n is the unity normal vector of the integration surface S, B is the magnetic field density, and μ_0 is the permeability of vacuum. In the 2D case, the integration path is a contour. The closed contour along the middle layer of the five–layer air gap mesh is used as an integration path.

• **Step 6:** The objective function and the penalties are found empirically. Their values are determined from **Step 3** through **Step 5**. The objective function is given by (13).

$$q = \frac{mF_0}{Fm_0} + p_1 + p_2 \qquad (13)$$

where m_0 and F_0 are the initial mass and the initial force of the bearing. m and F are the mass and the force for actual parameter values. p_1 and p_2 denote the penalties (14).

$$\begin{aligned} p_1 &= \frac{F_0}{F} \qquad \text{if} \quad F < F_0 \\ p_2 &= \frac{m}{m_0} \qquad \text{if} \quad m > m_0 \end{aligned} \qquad (14)$$

The value of the objective function is minimized in the optimization procedure. The optimization proceeds with **Step 2** until a minimal parameter variation step or a maximal number of evolutionary iterations is reached.

IV. Parameters calculation

The values of the force $F(x_0, i_{p0})$, the current gain k_i and the position stiffness k_x, which appear in the linearized force equation (7), have been determined for the optimized and for the non–optimized bearing. For this purpose the parametric descriptions of the bearing geometry and of the magnetic excitation were used. The FEM–based 2D calculations were performed for different values of rotor displacement and control current, as described in **Step 3** through **Step 5**. For each mentioned operating point $x = x_0$, $i_p = i_{p0}$, the current gain k_i has been calculated as the quotient of the force difference and the control current difference, and the position stiffness k_x has been calculated as the quotient of the force difference and the rotor displacement difference.

Special attention was focused on the calculation of force. A five–layer mesh was generated in the air gap. The closed contour along the middle air gap mesh layer, for all calculations at the same position with respect to the stator, was used as an integration path. The force was determined by Maxwell's stress tensor method.

The obtained results were checked in some points by FEM–based 2D calculations which were carried out by a commercial software package [8]. The forces were determined by the Virtual Work method. The differences between the forces calculated by Maxwell's stress tensor method and the Virtual Work method were smaller than one percent in all discussed cases.

V. Results

The data of the non–optimized and of the optimized bearing are given in Table I. The optimization has been performed in the operating point $x = 0$, $y = 0$, $i_p = i_b = 5$ A. All design parameters are rounded off to one tenth of a millimeter. The optimization data are given in Table II while the bearing geometry is shown in Fig. 2.

TABLE I
Data of the non–optimized and the optimized bearing

parameter	non–optimized	optimized
stator yoke s_y [mm]	8.5	7.2
rotor yoke r_y [mm]	9.0	7.8
leg width l_w [mm]	10.0	9.0
length of bearing l [mm]	53.0	56.3
mass of bearing m [kg]	2.691	2.688
force F [N]	580.01	629.74
objective function q	1	0.92

TABLE II
The optimization data

Optimization method	Differential Evolution
Number of parameters	4
Population size	20
Number of iterations	60

The objective function and the step–length ([6],[7]) during the optimization are shown in Fig. 3. The minimal value of the objective function has been reached after 43 iterations.

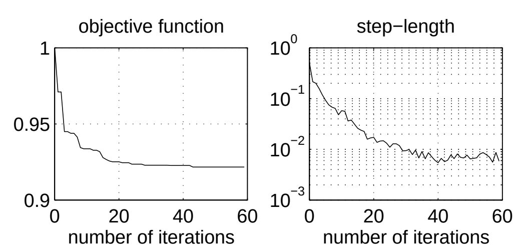

Fig. 3. The objective function and the step–length

The values of the force F, the current gain k_i and the position stiffness k_x (equation (7)) calculated for the optimized and for the non–optimized bearing by **Step 3**

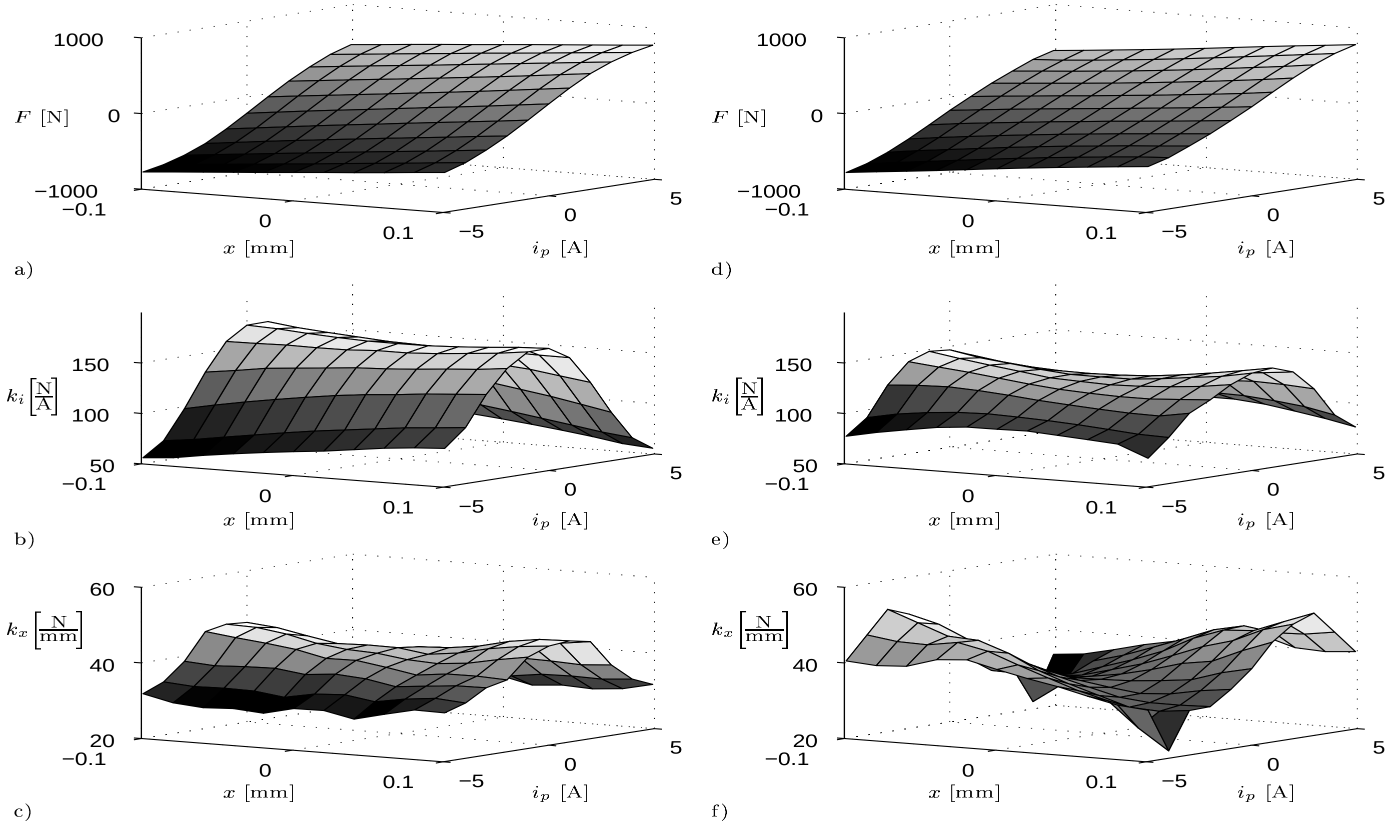

Fig. 4. Force F, current gain k_i and position stiffness k_x calculated in different operating points $i_p = i_{p0}$, $x = x_0$;
The optimized bearing: a) force F, b) current gain k_i, c) position stiffness k_x;
The non–optimized bearing: d) force F, e) current gain k_i, f) position stiffness k_x;

through **Step 5** are given for different values of the control current $i_p = i_{p0}$ and rotor displacement $x = x_0$ in Fig. 4.

The optimization results, given in Table I and by FEM calculated parameters of the optimized and of the non–optimized radial magnetic bearing compared in Fig. 4, show that the optimization has increased the maximal force of the radial bearing for more than 8.5 %, while the mass of the bearing has remained unchanged at a negligible increase of nonlinearities of the characteristics. The FEM calculations make it possible to determine the characteristics of the bearing model, and thereby to evaluate the dynamic properties and control algorithm of the entire AMBs system prior the prototype is made.

VI. Conclusion

The paper describes the optimization of a radial AMB and the determination of the bearing model parameters linearized about various operation points. It has been shown that the use of optimization methods in combination with the FEM can increase the maximum bearing force at an unchanged mass and a negligible increase of magnetic nonlinearities. By FEM–based 2D calculations the values of the force, position stiffness and current gain in different operating points of the optimized and non–optimized bearing have been determined. These results make it possible to evaluate the robustness of the control algorithm. Moreover, they can be approximated by a continuous function, which is further used for the linearization on the entire surface, and altogether applied in the synthesis of the nonlinear bearing control.

References

[1] Gerhard Schweitzer, Hannes Bleuler, and Alfons Traxler, *Active magnetic bearings*, Vdf Hochschulverlag AG an der ETH Zürich, ETH Zürich, 1994.

[2] Matti Antila, Erkki Lantto, and Antero Arkkio, "Determination of forces and linearized parameters of radial active magnetic bearings by finite element technique," *IEEE Transaction on Magnetics*, vol. 34, no. 3, pp. 684–694, 1998.

[3] Drago Dolinar, Gorazd Štumberger, and Bojan Grčar, "Calculation of the linear induction motor model parameters using finite elements," *IEEE Transaction on Magnetics*, vol. 34, no. 5, pp. 3640–3643, 1998.

[4] Pier Giorgio Alotto, Cela Eranda, Bernhard Brandstätter, Günter Fürntratt, Cristian Magele, Giorgio Molinari, Mario Nervi, Kurt Preis, Maurizio Repetto, and Kurt R. Richter, "Stochastic algorithms in electromagnetic optimization," *IEEE Transaction on Magnetics*, vol. 34, no. 5, pp. 3674–3684, 1998.

[5] Kay Hameyer, "Numerical optimization of finite element models in electromagnetics with global evolution strategy," in *Adaptive Computing in Engineering Control*, Plymouth,USA, 1994, pp. 61–66.

[6] R. Storn and K. Price, "Minimizing the real functions of the icec'96 contest by Differential Evolution," in *IEEE Conference on Evolutionary Computation*, Nagoya, Japan, 1996, IEEE, pp. 842–844, IEEE.

[7] Uwe Pahner, Ronny Mertens, Herbert De Gersem, Ronnie Belmans, and Kay Hameyer, "A parametric finite element environment tuned for numerical optimization," *IEEE Transaction on Magnetics*, vol. 34, no. 5, pp. 2936–2939, 1998.

[8] J. D. Edwards in E. M. Freeman, *Magnet 5.1 User Guide*. Infolytica Corporation Montreal: Infolytica, 1995.